

# Mesostructured Lamellar Phases Containing Six-Membered Vanadium Borophosphate Cluster Anions

Junghwan Do and Allan J. Jacobson\*

Department of Chemistry, University of Houston, Houston, Texas 77204-5641

Received January 18, 2001. Revised Manuscript Received April 27, 2001

A series of compounds with the general formula  $(\text{NH}_4)_x(\text{C}_n\text{H}_{2n+1}\text{NH}_3)_y[(\text{NH}_4)\text{V}_2\text{P}_2\text{BO}_{12}]_6 \cdot z\text{H}_2\text{O}$  ( $7 \leq n \leq 18$ ,  $x + y = 17$ ) was prepared by reaction of *n*-alkylamines with ammonium vanadium borophosphate,  $(\text{NH}_4)_{17}[(\text{NH}_4)\text{V}_2\text{P}_2\text{BO}_{12}]_6 \cdot 14\text{H}_2\text{O}$  ( $\text{NH}_4\text{-VBPO}$ ). The alkylammonium vanadium borophosphates (alkylammonium-VBPOs) were characterized by powder X-ray diffraction, IR spectroscopy, TEM analysis, thermogravimetric measurements, and elemental analysis. The results show that the structures of the alkylammonium-VBPO phases are composed of H-bonded layers of vanadium borophosphate cluster anions. Within the layers,  $\text{NH}_4$  cations and  $\text{H}_2\text{O}$  molecules are H-bonded either to the oxygen atoms of the cluster anions or to each other. The alkylammonium cations occupy the interlayer space and form either a bilayer with a chain orientation of  $\sim 47^\circ$  ( $7 \leq n \leq 12$ ) or an interdigitated arrangement with a chain orientation of  $\sim 90^\circ$  ( $13 \leq n \leq 18$ ).

## Introduction

Many layered oxides such as silicates, transition metal oxides, hydroxides, phosphates, and arsenates readily intercalate long-chain alkylamines. Some layered alkali transition metal oxides exchange alkali metal cations for alkylammonium ions directly.<sup>1</sup> Recently, interest in these inorganic–organic (surfactant) phases has dramatically increased in part because of the successful synthesis by Mobil of a family of silica-based mesoporous materials called M41S.<sup>2,3</sup> Similar phases formed from cluster anions and surfactants have been relatively less well studied, although several are known. Some recent examples related to the present work are summarized below.

In the structure of dodecylammonium thiostannate,  $[\text{Sn}_2\text{S}_6]^{4-}$  cluster anions form an infinite layer stabilized by H-bonds between neighboring ammonium cations and water molecules.<sup>4</sup> The alkyltrimethylammonium germanium sulfides contain similar layers of unconnected  $[\text{Ge}_4\text{S}_{10}]^{4-}$  cluster anions, separated by an interdigitated arrangement of alkyltrimethylammonium cations.<sup>5,6</sup> Interestingly, these compounds show absorption properties for linear alcohols of various chain lengths.

The cluster anion–surfactant phases have also been used as precursors for the assembly of mesoporous materials. The reaction of cetyltrimethylammonium germanium sulfide,  $\text{CTA}_4\text{Ge}_4\text{S}_{10}$ , with metal salts in

nonaqueous solution results in the formation of hexagonal metal germanium sulfide mesoporous structures in which the metal ions (Co, Ni, Cu, Zn) are coordinated to sulfur atoms in the  $[\text{Ge}_4\text{S}_{10}]$  cluster anions.<sup>7–9</sup> In an alternate synthetic route, the hydrothermal reaction of  $\text{Na}_4\text{Ge}_4\text{S}_{10}$ ,  $\text{MnCl}_2$ , and mesityltrimethylammonium bromide leads to the formation of a mesostructured manganese germanium sulfide with a hexagonal structure.<sup>10</sup> Cetyltrimethylammonium glycometalates form lamellar mesophases that, on hydrolysis, produce well-ordered mesoporous metal oxides.<sup>7,11,12</sup> Interdigitated arrangements of alkyl chains are found between H-bonded layers of dihydrogen phosphate anions in decylammonium dihydrogen phosphate.<sup>7,13,14</sup> Similar alkylammonium phosphate salts containing cyclopentylammonium and octylammonium cations between H-bonded layers of mono-dihydrogen phosphate anions have been reported.<sup>13</sup>

The water-soluble vanadium borophosphate compound  $(\text{NH}_4)_{17}[(\text{NH}_4)\text{V}_2\text{P}_2\text{BO}_{12}]_6 \cdot 14\text{H}_2\text{O}$  ( $\text{NH}_4\text{-VBPO}$ ), containing the cluster anion  $[(\text{NH}_4)\text{V}_2\text{P}_2\text{BO}_{12}]_6^{17-}$ , was first reported by us.<sup>14</sup> In this paper, we describe the results of the assembly of this anion with *n*-alkylammonium cations to form a series of lamellar compounds. Powder X-ray diffraction, infrared spectroscopy, TEM analysis, thermogravimetric measurements and elemental analysis were used to characterize compounds with

\* Author to whom correspondence should be addressed. Tel: (713) 743-2785. Fax: (713) 743-2787. E-mail: ajacob@uh.edu.

(1) Beneke, K.; Lagaly, G. Z. *Naturforsch.* **1978**, *33b*, 564.  
 (2) Kresge, C. T.; Leonowicz, M. E.; Roth, W. J.; Vartuli, J. C.; Beck, J. S. *Nature* **1992**, *359*, 710.  
 (3) Monnier, A.; Schuth, F.; Huo, Q.; Kumar, D.; Margolese, D.; Maxwell, R. S.; Stucky, G. D.; Krishnamurty, M.; Petroff, P.; Firouzi, A.; Janicke, M.; Chmelka, B. F. *Science* **1993**, *261*, 1299.  
 (4) Li, J.; Marler, B.; Kessler, H.; Soulard, M.; Kallus, S. *Inorg. Chem.* **1997**, *36*, 4697.  
 (5) Froba, M.; Oberender, N. *Chem. Commun.* **1997**, 1729.  
 (6) Bonhomme, F.; Kanatzidis, M. G. *Chem. Mater.* **1998**, *10*, 1153.

(7) Ozin, G. A. *Chem. Commun.* **2000**, 419.  
 (8) MacLachlan, M. J.; Coombs, N.; Ozin, G. A. *Nature* **1999**, *397*, 681.  
 (9) MacLachlan, M. J.; Coombs, N.; Bedard, R. L.; White, S.; Thompson, L. K.; Ozin, G. A. *J. Am. Chem. Soc.* **1999**, *121*, 12005.  
 (10) Rangan, K. K.; Billinge, S. J. L.; Petkov, V.; Heising, J.; Kanatzidis, M. G. *Chem. Mater.* **1999**, *11*, 2629.  
 (11) Khushalani, D.; Ozin, G. A.; Kuperman, A. *J. Chem. Mater.* **1999**, *9*, 1483.  
 (12) Khushalani, D.; Ozin, G. A.; Kuperman, A. *J. Chem. Mater.* **1999**, *9*, 1491.  
 (13) Oliver, S.; Lough, A.; Ozin, G. A. *Inorg. Chem.* **1998**, *37*, 5021.  
 (14) Bontchev, R.; Do, J.; Jacobson, A. J. *Angew. Chem., Int. Ed. Engl.* **1999**, *38*, 1937.

**Table 1. Optimized Synthetic Conditions for Alkylammonium-VBPO<sup>a</sup>**

| $C_n$           | alkylamine – solvent                             | temperature     |
|-----------------|--|-----------------|
| C <sub>7</sub>  | C <sub>7</sub> H <sub>17</sub> N – hexane        | RT <sup>b</sup> |
| C <sub>8</sub>  | C <sub>8</sub> H <sub>19</sub> N – hexane        | RT              |
| C <sub>9</sub>  | C <sub>9</sub> H <sub>21</sub> N – hexane        | RT              |
| C <sub>10</sub> | C <sub>10</sub> H <sub>23</sub> N – hexane       | 60 °C           |
| C <sub>11</sub> | C <sub>11</sub> H <sub>25</sub> N – hexane       | 60 °C           |
| C <sub>12</sub> | C <sub>12</sub> H <sub>27</sub> N·HCl – hexane   | RT              |
| C <sub>13</sub> | C <sub>13</sub> H <sub>29</sub> N – acetone      | RT              |
| C <sub>14</sub> | C <sub>14</sub> H <sub>31</sub> N + HCl – hexane | RT              |
| C <sub>15</sub> | C <sub>15</sub> H <sub>33</sub> N – hexane       | RT              |
| C <sub>16</sub> | C <sub>16</sub> H <sub>35</sub> N – hexane       | RT              |
| C <sub>17</sub> | C <sub>17</sub> H <sub>37</sub> N – hexane       | RT              |
| C <sub>18</sub> | C <sub>18</sub> H <sub>39</sub> N – hexane       | RT              |

<sup>a</sup> All reactions used 0.2779 g (0.1 mmol) of NH<sub>4</sub>-VBPO. <sup>b</sup> RT = room temperature.

the general compositions (NH<sub>4</sub>)<sub>x</sub>(C<sub>n</sub>H<sub>2n+1</sub>NH<sub>3</sub>)<sub>y</sub>[(NH<sub>4</sub>)<sub>2</sub>V<sub>2</sub>P<sub>2</sub>BO<sub>12</sub>]<sub>z</sub>·zH<sub>2</sub>O ( $x + y = 17$ ,  $7 \leq n \leq 18$ ).

### Experimental Section

**Synthesis.** The compounds were synthesized by two-step reactions. In the first step, (NH<sub>4</sub>)<sub>18</sub>[V<sub>2</sub>P<sub>2</sub>BO<sub>12</sub>]<sub>6</sub>·14H<sub>2</sub>O (NH<sub>4</sub>-VBPO) was prepared hydrothermally as previously reported.<sup>14</sup> V<sub>2</sub>O<sub>3</sub> (0.2248 g, 1.5 mmol), H<sub>3</sub>BO<sub>3</sub> (0.3090 g, 5 mmol), H<sub>3</sub>PO<sub>4</sub> (0.342 mL, 85 wt % solution in H<sub>2</sub>O, 5 mmol), NH<sub>4</sub>OH (2 mL, 29.6% solution in H<sub>2</sub>O, 15.4 mmol), and H<sub>2</sub>O (2 mL) were allowed to react at 160 °C. The resulting blue crystals of NH<sub>4</sub>-VBPO were used in the second step of the synthesis. The second reaction step is exemplified for heptylamine. The optimum reaction conditions to obtain single-phase products are summarized in Table 1.

As a typical example, the compound (NH<sub>4</sub>)(heptylamineH)<sub>17</sub>·[V<sub>2</sub>P<sub>2</sub>BO<sub>12</sub>]<sub>6</sub>·12H<sub>2</sub>O was synthesized by the following procedure. Heptylamine (0.1 mL, 0.67 mmol) in hexane (10 mL) was slowly added to a solution of (NH<sub>4</sub>)<sub>18</sub>[V<sub>2</sub>P<sub>2</sub>BO<sub>12</sub>]<sub>6</sub>·14H<sub>2</sub>O (0.277 g, 0.1 mmol) in H<sub>2</sub>O (20 mL). The mixture was stirred for 2 h at room temperature. The blue aggregated powder product was filtered, washed with distilled water, and dried at room temperature. Similar reaction conditions were used for the other compounds.

**Characterization.** The compositions of the products were determined by a combination of thermogravimetric (SDT 2960 DTA-TGA, TA Instruments) and elemental analysis (Galbraith Laboratories, Knoxville, TN). TGA measurements were made in air at a scan rate of 2 °C/min to 800 °C. Interlayer spacings were determined from X-ray diffraction data recorded on a Scintag XDS 2000 automated diffractometer in  $\theta$ - $\theta$  geometry with Cu K $\alpha$  radiation ( $\lambda = 1.5406$  Å). The infrared spectra (KBr pellet method) were recorded on a Galaxy FTIR 5000 series spectrometer. The transmission electron microscope (TEM) employed in this work was a JEOL 2000 FX instrument.

### Results

**Synthesis and Powder-XRD Analysis.** The reaction of NH<sub>4</sub>-VBPO with  $n$ -alkylamines leads to the formation of alkylammonium-VBPO phases. Selected powder X-ray diffraction patterns of C<sub>16</sub>- and C<sub>18</sub>-VBPO are shown in Figure 1. The first three strong (00 $l$ ) peaks ( $l = 1, 2, 3$ ) at low angles are indicative of the lamellar mesostructures of the compounds. In Figure 1, the intensities are plotted on a logarithmic scale to emphasize the weak reflections. The observed interlayer spacings are determined by the packing of the hydrocarbon chains of the alkylammonium cations in the interlayer space. The interlayer spacings of each product are presented in Table 2. For the compounds with  $10 \leq n \leq 14$ , two interlayer spacings are shown for reasons

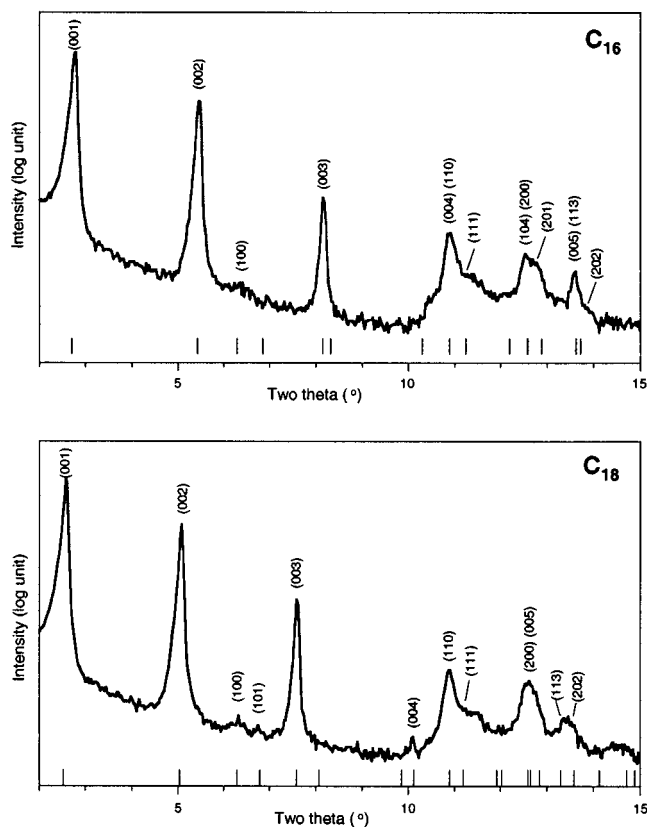


**Figure 1.** X-ray powder diffraction patterns of C<sub>16</sub>- and C<sub>18</sub>-VBPO. The intensity data are given on a logarithmic scale.

**Table 2. Interlayer Spacings and CH<sub>2</sub> Asymmetric Stretching Vibrations for Alkylammonium-VBPO**

| $n$             | interlayer spacing (Å) <sup>a</sup> | CH <sub>2</sub> vibration (cm <sup>-1</sup> ) |
|-----------------|-------------------------------------|---|
| 7               | 24.15                               | 2928  |
| 8               | 26.10                               | 2926  |
| 9               | 27.55                               | 2924  |
| 10 <sup>b</sup> | 29.86                               | 2922  |
|                 | 28.17                               |   |
| 11 <sup>b</sup> | 31.61                               | 2922  |
|                 | 28.36                               |   |
| 12 <sup>b</sup> | 33.38                               | 2920.5  |
|                 | 27.51                               |   |
| 13 <sup>b</sup> | 28.64                               | 2920.5  |
|                 | 35.14                               |   |
| 14 <sup>b</sup> | 29.99                               | 2920.5  |
|                 | 38.50                               |   |
| 15              | 31.04                               | 2920.5  |
| 16              | 32.53                               | 2918.5  |
| 17              | 34.16                               | 2918.5  |
| 18              | 34.97                               | 2918.5  |

<sup>a</sup> Interlayer spacings are obtained from (003) reflections. <sup>b</sup> Two-phase mixtures are prepared in hexane at room temperature and differently treated to obtain single phases (see Table 1).

discussed below. The observed interlayer spacings for all compounds can be divided into two distinct regions showing the differences in the relative importance of chain packing and van der Waals' interactions between chains (Figure 2).

The compounds from C<sub>8</sub> to C<sub>9</sub> and from C<sub>15</sub> to C<sub>18</sub> were obtained as single phases in hexane at room temperature. For the C<sub>10</sub>–C<sub>14</sub> compounds, two-phase mixtures were obtained by using the same reaction conditions. For C<sub>10</sub> and C<sub>11</sub>, one phase has an interlayer spacing that lies on the extrapolation of line i in Figure 2, but the other phase has a smaller spacing (see Table 2 and

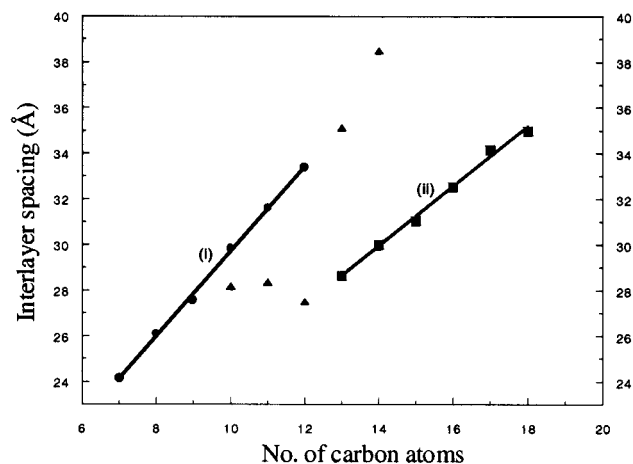


**Figure 2.** Interlayer spacing vs number of carbon atoms in alkyl chain for the  $(\text{NH}_4)_x(\text{C}_n\text{H}_{2n+1}\text{NH}_3)_y[(\text{NH}_4)\text{VO}_2\text{P}_2\text{BO}_{12}]_6 \cdot z\text{H}_2\text{O}$  phases. The filled triangles indicate the interlayer spacing of the minor phase observed in  $\text{C}_{10}$ – $\text{C}_{14}$  reactions.

Figure 2). Pure phases of the  $\text{C}_{10}$  and  $\text{C}_{11}$  compounds (upper line) were prepared by heating the reactants at  $60^\circ\text{C}$  for 2 h. For  $\text{C}_{12}$  and  $\text{C}_{13}$ , the two interlayer spacings lie on lines i and ii. For  $\text{C}_{12}$ , a pure phase with the higher interlayer spacing (line i) was obtained by using  $\text{C}_{12}\text{H}_{27}\text{N}\cdot\text{HCl}$  as one of the reactants. A single-phase product with an interlayer spacing that lies on the extrapolation of line ii could not be obtained by varying the reaction conditions. The  $\text{C}_{13}$  phase with the larger spacing was not observed when the solvent was changed to acetone. However, a single phase containing only the shorter spacing on line ii cannot be synthesized, even though a larger amount of the phase can be obtained by heating the solution. For the  $\text{C}_{14}$  compound, one of the phases has a longer spacing than expected from the extrapolation of line i. A single phase of the  $\text{C}_{14}$  compound with the line ii spacing was obtained by adding a drop of concentrated HCl.

**Compositional Study (TGA and Elemental Analysis).** Thermogravimetric analysis results show that the evolution of crystal water,  $\text{NH}_3$ , carbon oxides, and  $\text{H}_2\text{O}$  molecules from the structure and the oxidation of  $\text{V}^{4+}$  to  $\text{V}^{5+}$  are completed between  $\sim 600$  and  $\sim 700^\circ\text{C}$  in several steps. For the longer alkylammonium chains, the evolution of water occurs below  $100^\circ\text{C}$ . The weight remains constant until  $\sim 200^\circ\text{C}$ , where decomposition begins. A typical TGA curve of  $\text{C}_{18}$ -VBPO is shown in Figure 3. The compounds with shorter alkylammonium chains ( $n < 12$ ) decompose over a wider temperature range without distinct steps. The compositions of each compound as determined by elemental analysis and TGA measurements are shown in Table 3.

**IR Spectroscopy.** Selected IR spectra are shown in Figure 4. The characteristic infrared spectra in the region of  $1200$ – $400\text{ cm}^{-1}$ , corresponding to  $\text{V}=\text{O}$ ,  $\text{P}-\text{O}$ , and  $\text{B}-\text{O}$  vibrations, confirm the presence of  $[(\text{NH}_4)\text{VO}_2\text{P}_2\text{BO}_{10}]_6$  cluster anions. The positions of the  $\text{CH}_2$  asymmetric stretching vibrations in the IR spectra provide information on the extent to which the alkyl chains of the alkylammonium cations have crystalline or liquidlike structures. The IR spectra of a well-ordered trans configuration and a disordered gauche defect structure show bands at  $\sim 2918\text{ cm}^{-1}$  and above  $2925\text{ cm}^{-1}$ , respectively. In the alkylammonium-VPBO

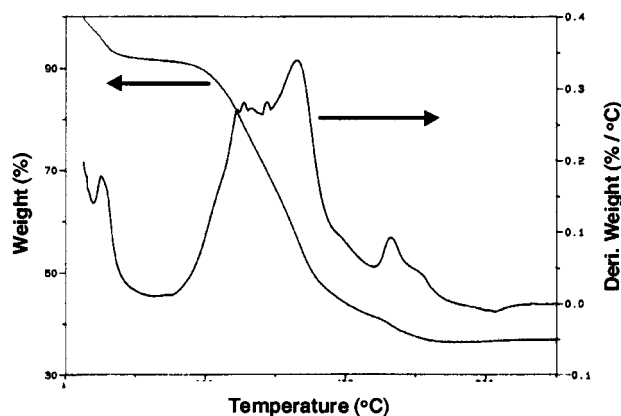


**Figure 3.** Thermogravimetric analysis data for  $\text{C}_{18}$ -VBPO.

**Table 3. Compositions of the Alkylammonium-VPBO Compounds Based on Elemental Analysis and TGA<sup>a</sup>**

|                 | V  | y    | N    | y (z) (based on TGA) <sup>b</sup> |
|-----------------|----|------|------|-----------------------------------|
| $\text{C}_7$    | 12 | 15.9 | 17.0 | $\leq 17$                         |
| $\text{C}_8$    | 12 | 15.7 | 18.8 | $\leq 16$                         |
| $\text{C}_9$    | 12 | 14.4 | 18.6 | $\leq 14$                         |
| $\text{C}_{10}$ | 12 | 16.2 | 18.6 | $\leq 15$                         |
| $\text{C}_{11}$ | 12 | 16.6 | 19.2 | $\leq 16$                         |
| $\text{C}_{12}$ | 12 | 15.5 | 18.2 | 16 (z = 31)                       |
| $\text{C}_{13}$ | 12 | 12.5 | 19.9 | 14 (z = 21)                       |
| $\text{C}_{14}$ | 12 | 13.2 | 18.9 | 12 (z = 21)                       |
| $\text{C}_{15}$ | 12 | 12.3 | 18.9 | 12 (z = 18)                       |
| $\text{C}_{16}$ | 12 | 13.7 | 19.9 | 13 (z = 26)                       |
| $\text{C}_{17}$ | 12 | 13.5 | 19.0 | 12 (z = 19)                       |
| $\text{C}_{18}$ | 12 | 13.3 | 19.2 | 12 (z = 21)                       |

<sup>a</sup> The left three columns show the calculated mole ratios relative to 12 vanadium atoms in  $(\text{NH}_4)_x(\text{C}_n\text{H}_{2n+1}\text{NH}_3)_y[(\text{NH}_4)\text{VO}_2\text{P}_2\text{BO}_{12}]_6 \cdot z\text{H}_2\text{O}$  ( $x + y = 17$ ,  $7 \leq n \leq 18$ ). <sup>b</sup> The water contents (z values) for compounds with  $n \geq 12$  were obtained assuming that the evolution of water occurs below  $100^\circ\text{C}$ .

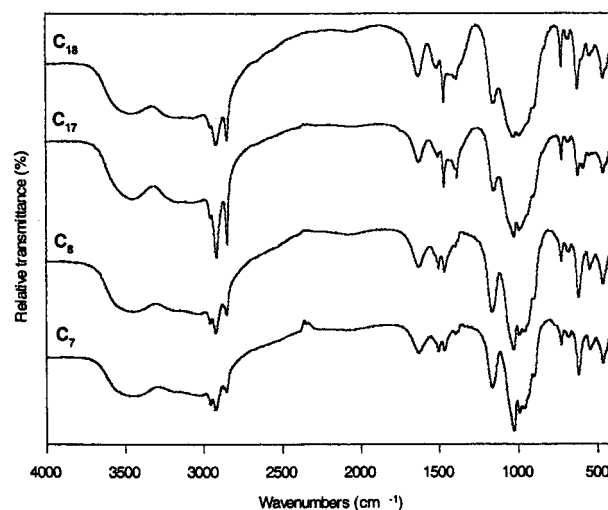


**Figure 4.** Representative infrared spectra for the alkylammonium-VPBO phases.

compounds, as the alkyl chain length increases, the wavenumber of the  $\text{CH}_2$  asymmetric stretching vibration gradually decreases to  $2918.5\text{ cm}^{-1}$ , indicating that, as  $n$  increases, the chains become more ordered and closer packed.

## Discussion

The interlayer spacing increases as the number of carbon atoms in the alkyl chains is increased (Figure



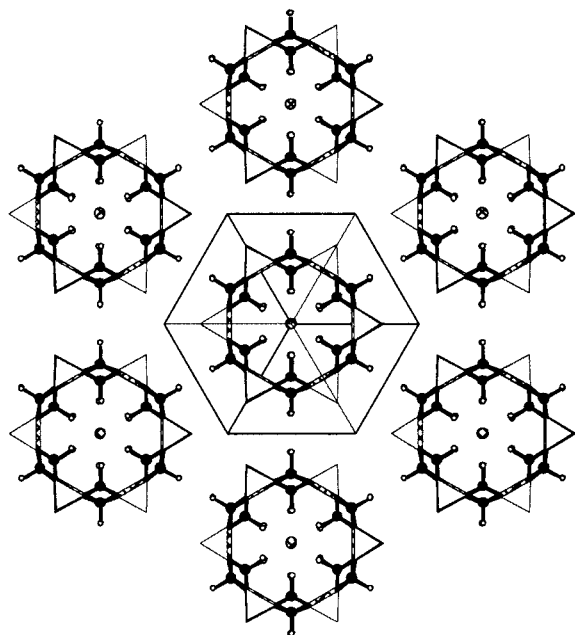


**Figure 5.** Layers of six-membered vanadium borophosphate cluster anions in  $NH_4$ -VPBO. The  $PO_4$  and  $BO_4$  units are shown as filled and crosshatched tetrahedra, respectively, the vanadium and oxygen atoms as filled and open circles, respectively, and the nitrogen atoms as crosshatched circles.

2). In region i, a least-squares fit to the data gives

$$d = 1.856n + 11.141 \text{ \AA}$$

where  $d$  is the interlayer spacing and  $n$  is the number of carbon atoms in the alkylammonium cations. The increment of 1.856 Å per carbon atom implies bilayer arrangements of the alkylammonium cations between the layers. The slope of this line gives the mean angle  $\alpha$  that the chains make with the layer surface by the relation  $\alpha = \sin^{-1}[1.856/(1.27 \times 2)] = 46.9^\circ$ , where 1.27 Å is the length increment per carbon atom in a linear all-trans chain.

In region ii, a least-squares fit to the data gives

$$d = 1.304n + 11.666 \text{ \AA}$$

If the molecules in this region have the same bilayer arrangement of alkylammonium cations as do those in region i, then the tilt angle should be  $\alpha = 30.9^\circ$ , which is indicative of weaker van der Waals' interactions between the alkylammonium cations than in region i. However, in general, as the chain length increases, the van der Waals' interactions also increase, which should result in a more ordered arrangement and a substantial increase of the tilt angle  $\alpha$ . Thus, an interdigitated arrangement is more likely in region ii with a perpendicular direction of chains,  $\alpha \approx 90^\circ$ . This model is supported by the infrared data, which indicate that, for  $C_{16}$ – $C_{18}$ , the alkyl chains adopt an all-trans configuration (observed  $CH_2$  asymmetric stretching vibration, 2918  $cm^{-1}$  for  $C_{16}$ ,  $C_{17}$ , and  $C_{18}$ ).

Previously reported VBPOs, such as  $NH_4$ VPBO (Figure 5), have layer structures in which  $NH_4^+$  and  $H_2O$  are H-bonded either to the oxygen atoms of the cluster anions or to each other.<sup>14–16</sup> In the X-ray data for the

alkylammonium-VPBO compounds, several weak reflections indicate a similar hexagonal arrangement (Figure 5). For  $C_{18}$ -VBPO, assuming that the next peak after the  $(00l)$  ( $l = 1, 2, 3, 4$ ) peaks corresponds to the  $(110)$  reflection, the other observed peak positions are in good agreement with those calculated for the hexagonal cell parameters  $a = 16.22(1)$  Å and  $c = 34.968(5)$  Å. Between  $(002)$  and  $(003)$ , two additional small peaks corresponding to the  $(100)$  and  $(101)$  reflections are observed. Also, the lines in the X-ray powder diffraction pattern of  $C_{16}$ -VBPO are well indexed when the same value of  $a = 16.22$  Å is used but with a smaller value of  $c = 32.526$  Å (Figure 1). In the other alkylammonium-VBPO phases, the same lattice parameter,  $a = 16.22$  Å, is observed independent of the chain lengths of the alkylamines in the structures. The hexagonal lattice parameter ( $a = 16.22$  Å) is in good agreement with the lattice parameter  $a = 16.5490(9)$  Å observed in  $NH_4$ -VBPO (Figure 5).

Extrapolation of the data to  $n = 0$  gives intercepts of 11.141 and 11.666 Å for regions i and ii, respectively. The values are larger than the value of 10.36 Å observed for the interlayer distance between H-bonded  $[(NH_4)\Delta V_2P_2BO_{12}]_6^{17-}$  layers in  $NH_4$ -VBPO.<sup>14</sup> The increase might reflect some buckling of the layers of the alkylammonium-VBPO phases caused by the interactions between the alkyl chains in the alkylammonium cations. The smaller  $a$  value is also consistent with some layer distortion.

The effective interlayer areas per alkyl chain based on the structure of  $NH_4$ -VBPO are 29.8 and 39.7 Å<sup>2</sup>, assuming that the compounds in regions i and ii have general compositions of  $(NH_4)_2(\text{alkylamineH})_{16}[V_2P_2BO_{12}]_6 \cdot zH_2O$  and  $(NH_4)_6(\text{alkylamineH})_{12}[V_2P_2BO_{12}]_6 \cdot zH_2O$ , respectively. The linear all-trans hydrocarbon chain in polyethylene has a cross-sectional area of 18.2 Å<sup>2</sup>. The cross-sectional area of 39.7 Å<sup>2</sup> in region ii is almost twice the value of 18.2 Å<sup>2</sup> in polyethylene, which strongly supports an interdigitated configuration with a perpendicular orientation of the chains.<sup>17</sup>

The increase in layer spacing observed when the alkylammonium chain length is increased by one carbon is plotted as interlayer spacing vs carbon number (Figure 2). Jacobson et al. showed that a regular odd–even alteration in interlayer spacing is a consequence of a perpendicular orientation of the C–N bond and a chain angle of  $\sim 68^\circ$  with respect to the layers.<sup>18</sup> However, in this case no odd–even alteration is apparent in either region i or region ii, consistent with the disorder in region i and the  $90^\circ$  chain orientation in region ii.

The electron microscopy results are consistent with the data obtained from X-ray diffraction. A TEM image of the  $C_{15}$ -VBPO compound is shown in Figure 6. The figure shows a layered structure with a layer separation of ca. 32 Å, in agreement with the  $d$  spacing calculated from the X-ray diffraction data. Also, the thickness of the layer is approximately 10 Å, in excellent agreement with the calculated thickness of  $[(NH_4)\Delta V_2P_2BO_{12}]_6$

(16) Do, J.; Bontchev, R.; Jacobson, A. J. *Inorg. Chem.* **2000**, *39*, 3230.

(17) Pechold, W.; Liska, E.; Grossman, H. P.; Hagele, P. C. *Pure Appl. Chem.* **1976**, *46*, 127.

(18) Jacobson, A. J.; Johnson, J. W.; Lewandowski, J. T. *Mater. Res. Bull.* **1987**, *22*, 45.

(15) Do, J.; Zheng, L.; Bontchev, R.; Jacobson, A. J. *Solid State Sci.* **2000**, *2*, 343.

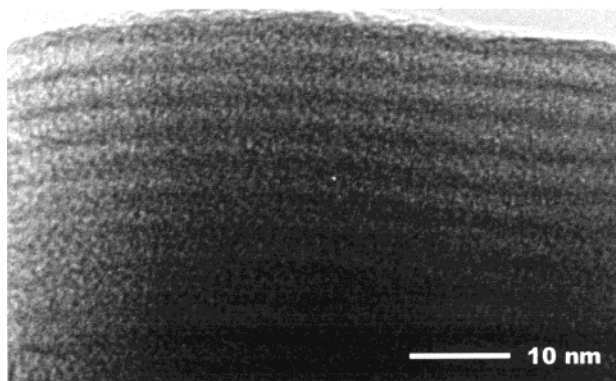


**Figure 6.** Transmission electron micrograph of C<sub>15</sub>-VBPO.

cluster anions. The TEM results confirm the lamellar structure of the alkylammonium-VBPO phases.

In summary, a series of compounds with the general formula  $(\text{NH}_4)_x(\text{C}_n\text{H}_{2n+1}\text{NH}_3)_y[(\text{NH}_4)\text{V}_2\text{P}_2\text{BO}_{12}]_6 \cdot z\text{H}_2\text{O}$  ( $7 \leq n \leq 18$ ) was prepared by ion-exchange reactions of *n*-alkylamines with NH<sub>4</sub>-VBPO. Ammonium cations between the cluster anions are either fully or partially exchanged by *n*-alkylammonium cations immediately upon reaction. The XRD data reveal that the structures of alkylammonium-VBPO phases consist of H-bonded layers of vanadium borophosphate cluster anions in a hexagonal arrangement, between which the alkylammonium cations either lie in a bilayer with a chain orientation of  $\sim 47^\circ$  ( $7 \leq n \leq 12$ ) or are interdigitated with a chain orientation of  $\sim 90^\circ$  ( $13 \leq n \leq 18$ ). The different packings of the alkylammonium cations are

determined by the interactions between the alkyl chains, and the transition between two different packing arrangements occurs between C<sub>12</sub>- and C<sub>13</sub>-VBPO.

The alkylammonium-VBPO phases become less soluble with increasing *n*. Thus, NH<sub>4</sub>-VBPO is water-soluble, whereas C<sub>7</sub>-VBPO is not soluble in water but dissolves in either THF/water or acetone/water. Thus far, we have not been successful in growing single crystals from solution suitable for X-ray diffraction.

In conclusion, we have demonstrated that well-ordered lamellar mesophases can be obtained from large inorganic cluster anions and alkylammonium cations. We are at present investigating the use of other surfactants and coupling agents to form similar mesostructures with permanent porosity.

**Acknowledgment.** This work was supported by the National Science Foundation under Grant DMR-9805881 and by the Robert A. Welch Foundation. The work made use of MRSEC/TCSUH Shared Experimental Facilities supported by the National Science Foundation under Award DMR-9632667 and the Texas Center for Superconductivity at the University of Houston. We thank Prof. T. Randall Lee for his helpful discussions and Dr. I. A. Rusakova for the TEM measurements and for providing Figure 6.

**Supporting Information Available:** Tables of elemental analysis results, observed IR vibration modes, and X-ray powder patterns for all the compounds (PDF). This material is available free of charge via the Internet at <http://pubs.acs.org>.

CM010044M